

Single Particle Jumps in a Binary Lennard-Jones System Below The Glass Transition

K. Vollmayr-Lee*

Department of Physics, Bucknell University, Lewisburg, Pennsylvania 17837, USA

(Dated: November 21, 2018)

We study a binary Lennard-Jones system below the glass transition with molecular dynamics simulations. To investigate the dynamics we focus on events (“jumps”) where a particle escapes the cage formed by its neighbors. Using single particle trajectories we define a jump by comparing for each particle its fluctuations with its changes in average position. We find two kinds of jumps: “reversible jumps,” where a particle jumps back and forth between two or more average positions, and “irreversible jumps,” where a particle does not return to any of its former average positions, i.e. successfully escapes its cage. For all investigated temperatures both kinds of particles jump and both irreversible and reversible jumps occur. With increasing temperature relaxation is enhanced by an increasing number of jumps, and growing jump lengths in position and potential energy. However, the waiting time between two successive jumps is independent of temperature. This temperature independence might be due to aging, which is present in our system. The times of jump duration are at all temperatures significantly shorter than the waiting times. The ratio of irreversible to reversible jumps is also increasing with increasing temperature, which we interpret as a consequence of the increased likelihood of changes in the cages, i.e. a blocking of the “entrance” back into the previous cage. In accordance with this interpretation, the fluctuations both in position and energy are increasing with increasing temperature. A comparison of the fluctuations of jumping particles and non-jumping particles indicates that jumping particles are more mobile even when not jumping. The jumps in energy normalized by their fluctuations are decreasing with increasing temperature, which is consistent with relaxation being increasingly driven by thermal fluctuations. In accordance with subdiffusive behavior are the distributions of waiting times and jump lengths in position.

PACS numbers: 02.70.Ns, 05.20.-y, 61.20.Lc, 61.43.Fs, 64.70-Pf

I. INTRODUCTION

If a liquid is cooled and crystallization is avoided, one obtains a Supercooled liquid. Upon further cooling the system falls out of equilibrium and results in a glass. During the transition from liquid to supercooled liquid to glass the thermodynamic properties change and even more drastic changes occur in the dynamics [1]. The viscosity increases by many orders of magnitude upon cooling and the mean square displacement (MSD) as a function of time develops a plateau at intermediate times. The lower the temperature the longer the waiting time within the plateau until a second rise in the mean square displacement occurs [2]. One common explanation for the plateau is that while at high temperatures one has (at late enough times) normal diffusion, at lower temperatures particles are caged in, i.e. trapped by their neighbors, and spend longer time within this cage with decreasing temperatures. The second increase in the MSD indicates that after long enough waiting time the particles manage to escape their cage. This escape out of the cage (“jump”) is the focus of this paper.

To set the work of this paper in context, we review briefly previous studies on the dynamics of supercooled liquids and glasses. We restrict ourselves mostly to simple glass formers, excluding major work about strong glass formers, ionic systems, polymers and crystals.

Central quantities in both **experiments and computer simulations** are the viscosity, diffusion constant and MSD. The MSD, which is an average over single particle $i = 1, \dots, N$ displacements,

$$r^2(t) = \frac{1}{N} \sum_i |\mathbf{r}_i(t) - \mathbf{r}_i(0)|^2, \quad (1)$$

and variations thereof [3]

$$\Delta R(t) = (N \cdot \text{MSD})^{-1/2} \quad (2)$$

$$\Delta \overline{R(t)} = \left(\sum_i \langle |\mathbf{r}_i(t) - \mathbf{r}_i(0)|^2 \rangle_{\Delta t} \right)^{-1/2} \quad (3)$$

where $\langle \cdot \rangle_{\Delta t}$ is a time average

$$\Delta R^0(t) = \left(\sum_i |\mathbf{r}_i^0(t) - \mathbf{r}_i^0(0)|^2 \right)^{-1/2} \quad (4)$$

where $\mathbf{r}_i^0(t)$ is the position after steepest decent

show jumps when viewed with fine enough time resolution, and when studied at low enough temperatures and for single configurations [3, 4, 5, 6, 7, 8, 9, 10]. Detailed studies of these jumps indicate collective motion [3, 4, 5, 6].

One learns about the interplay between regular diffusion and hopping motion via four-point correlation functions [11, 12, 13, 14, 15] and the van Hove correlation function $G(r, t) = G_s(r, t) + G_d(r, t)$ [15, 16, 17, 18, 19, 20, 21, 22, 23, 24] where $G_s(r, t)$ is the self part and $G_d(r, t)$ is the distinct part. The hopping shows up in an

*Electronic address: kvollmay@bucknell.edu

additional peak in $G_s(r, t)$ and an increase in the amplitude at $r \rightarrow 0$ of $G_d(r, t)$.

Recently attention has been drawn to the non-Gaussian tail of $G(r, t)$ [25, 26, 27, 28] and the non-Gaussian parameter α_2 [5, 13, 25, 28, 29, 30, 31, 32, 33, 34] which is the second coefficient of the cumulant series of $F_s(q, t)$, the Fourier transform of $G_s(r, t)$. They are signatures of non-exponential behavior, which might be either due to homogeneous complex dynamics and/or due to spatially heterogeneous dynamics [35]. This has been studied both with experiments [28, 29, 30, 36] and in simulations of two-dimensional [31, 37, 38, 39, 40] and three-dimensional systems [3, 5, 6, 11, 25, 26, 27, 32, 40, 41, 42, 43, 44, 45, 46]. Studies of the most mobile particles reveal that they move increasingly more collectively with decreasing temperature. One distinct feature of this collective dynamics is that some particles are moving along a string [3, 8, 26, 30, 46, 47, 48].

Similar motion has been found via the study of normal modes which are commonly used to study the dynamics at low temperatures [8, 44, 45, 46, 47, 48, 49].

The dynamics of glasses out of equilibrium, i.e. systems which have been quenched from high to low temperature, displays additional complexity, since the system might “age” [50]. This means that the dynamics depends on the waiting time between the quench and the measurement [51, 52, 53] which results in the violation of the fluctuation dissipation theorem [53, 54].

Another fruitful approach to gain insight into the dynamics of supercooled liquids and glasses has been to investigate the energy landscape of the inherent structure, that means of the instantaneous configurations which have been quenched to their local potential energy minimum [14, 55, 56, 57, 58, 59, 60]. At the same temperature when the system starts slowing down drastically, the potential energy of the inherent structure undergoes a qualitative change [55]. The long time behavior of this potential energy shows jumps between metabasins, where the latter are groups of strongly correlated local minima [56, 57, 58, 59, 60]. The mean average waiting time $\langle \Delta t_{\text{wait}} \rangle$ between these jumps turns out to be dominated by the long times. $\langle \Delta t_{\text{wait}} \rangle$ together with the diffusion constant allow an estimate of the cage size [59].

Direct studies of the cage have been done via three-time correlations [14], velocity-velocity correlations [30, 38, 61], via the cage correlation function [62, 63, 64], and a passage time before a particle escapes [65]. The results of these studies tell us about cage properties such as the cage size and waiting time within a cage (or jump rate).

Hand in hand with the experiments and simulations are the **theoretical models** for supercooled liquids and glasses. One of the very successful theories is the mode coupling theory of the glass transition (MCT) [66], which describes the dynamics of supercooled liquids via non-linear dynamics of coupled density modes and makes predictions for quantities such as D , $F(q, t)$, and the susceptibility $\chi''(\omega)$. The extended version of MCT includes hopping processes via the coupling to current fluctuations

[67]. The comparison of experiment and this theory for $\chi''(\omega)$ [68] and α_2 [69] shows very good agreement.

The MCT is a theory for the glass transition for temperatures above the glass transition. Below the glass transition there exists no equivalent of a microscopic theory such as MCT. Some phenomenological theories which are more general models for solids build in hopping either indirectly as in the free volume model [70] or directly in hopping models [71, 72, 73]. Direct hopping models are based on the assumption that hopping is the main process which explains the dynamics. The starting point in these models is usually a random walk and the anomalous diffusion is incorporated via a distribution of waiting times (or jump rates). The jumping entities are either defects [71], uncharged carriers [72] or (in the case of predictions for ac and dc conductivity) charged carriers [73].

The goal of this paper is to obtain via single particle trajectories direct information about jump processes such as jump sizes and waiting times between jumps. Specific examples of the dynamics of single particle jumps, in the form of a plot of one component of $\mathbf{r}_i(t)$ [16, 17, 18, 74] or in the form of a two- or three-dimensional picture of the particle trajectory [6, 28, 29, 30, 31, 40, 57, 61], are very helpful to get an idea of some qualitative features of jumps, such as the detailed geometry of jump processes [16, 17, 57, 74]. In this paper, however, we go beyond single examples by defining a systematic search algorithm for jump processes. For the case of single particle trajectories a similar approach has been used in the work [17, 19, 34, 43], where the jump criterion is a minimum hopping distance, which is the same for all particles. In contrast, we use a relative criterion, where for each particle its size of fluctuations is compared to its jump size. We choose this relative criterion to be able to identify jumps of particles of different sizes and neighborhood. That means the criterion is adjusted to the cage size of each individual particle. As criterion for the occurrence of a jump we use the positions of particles instead of their energy. While both approaches are fruitful, we believe that many theoretical models and interpretations of simulations and experiments are based on an intuitive picture of the particle motion in real space. Similarly our goal is to mimic a careful observer of each particles motion in our system. We therefore use single particle trajectories, instead of a quantity which is an average over all particles (as in the work [3, 4, 5, 6, 7, 8, 9, 10]). For the case of single particle trajectories the distinction between vibrational and hopping motion turns out to be clearer by taking time averages than by using trajectories of the inherent structure.

In the following we define our model, and give details about the simulation (Sec. II). Our precise definition of a jump is given in Sec. III. We find two types of jumps (irreversible and reversible). The latter are distinguished for the rest of the paper (in distinction from [17, 19, 34, 43].) In Sec. IV we count as a function of temperature the number of jumping particles, and in Sec. V the number of visited different cages. In Sec. VI we investigate the

times during a jump and between successive jumps. The jump size both in position and in potential energy are presented in Secs. VII and VIII. In Sec. IX we conclude with a summary of our results, a comparison with the results of previous work and with our resulting picture of jump processes. We finish with open questions suggesting future work.

II. MODEL AND SIMULATION

We use a binary Lennard-Jones (LJ) mixture of 800 A and 200 B particles with the same mass. The interaction potential for particles i and j at positions \mathbf{r}_i and \mathbf{r}_j and of type $\alpha, \beta \in \{A, B\}$ is

$$V_{\alpha\beta}(r) = 4\epsilon_{\alpha\beta} \left(\left(\frac{\sigma_{\alpha\beta}}{r} \right)^{12} - \left(\frac{\sigma_{\alpha\beta}}{r} \right)^6 \right), \quad (5)$$

where $r = |\mathbf{r}_i - \mathbf{r}_j|$ and $\epsilon_{AA} = 1.0, \epsilon_{AB} = 1.5, \epsilon_{BB} = 0.5, \sigma_{AA} = 1.0, \sigma_{AB} = 0.8$ and $\sigma_{BB} = 0.88$. We truncate and shift the potential at $r = 2.5\sigma_{\alpha\beta}$. From previous investigations [75, 76] it is known that this system is not prone to crystallization and demixing. In the following we will use reduced units where the unit of length is σ_{AA} , the unit of energy is ϵ_{AA} and the unit of time is $\sqrt{m\sigma_{AA}^2/(48\epsilon_{AA})}$.

We carry out molecular dynamics (MD) simulations using the velocity Verlet algorithm with a time step of 0.02. The volume is kept constant at $V = 9.4^3 = 831$ and we use periodic boundary conditions. According to previous simulations [54, 75, 76] the kinetic glass transition is around $T \approx 0.435$. We analyze here simulations at $T = 0.15/0.2/0.25/0.30/0.35/0.38/0.40/0.41/0.42$ and 0.43 as they have been described in [42]. We start with 10 independent well equilibrated configurations at $T = 0.446$. [77] Each of these configurations undergoes the following sequence of simulation runs. After an instantaneous quench to $T = 0.15$ we first run a (NVT) simulation for 10^5 MD steps. The temperature is kept constant by replacing the velocities of all particles by new velocities drawn from the corresponding Boltzmann distribution every 50 time steps. We then run the simulation for 10^5 MD steps without the temperature bath (NVE) and subsequently raise the temperature instantaneously to the next higher temperature $T = 0.2$. (NVT) and (NVE) runs of 10^5 MD steps each follow and the temperature is again raised, and so forth. The final configurations of these (NVT) runs are the initial configurations for the (NVE) production runs (for $5 \cdot 10^6$ MD steps) presented in this paper. During each production run the positions of all particles (configurations) are stored every 2000 MD steps which are then used for analysis.

For the here investigated temperatures the relaxation times τ are much larger than the waiting time before the production runs (at $T = 0.446$ is $\tau \approx 8 \cdot 10^5$). We therefore study relaxation processes out of equilibrium and find aging effects, which is consistent with previous

detailed studies of aging of the same binary Lennard-Jones system [53, 54].

III. DEFINITION OF JUMP AND JUMP-TYPE

We focus in this paper on the process of a particle escaping its cage, using single particle trajectories $\mathbf{r}_i(t)$ given by the periodically stored configurations.

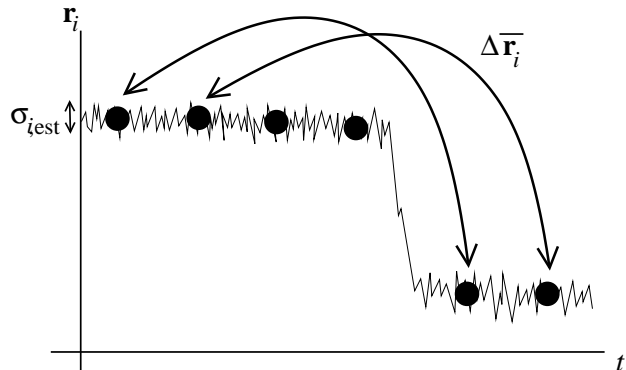


FIG. 1: Sketch of a particle trajectory to illustrate the definition of a jump by comparison of the fluctuations of the particle $\sigma_{i,\text{est}}$ and the difference in average positions $|\Delta \bar{\mathbf{r}}_i|$.

To distinguish vibrations around an average position from a change in the average position, we average 20 consecutive positions $\mathbf{r}_i(t)$ to obtain $\bar{\mathbf{r}}_i(m)$ as sketched in Fig. 1. We identify jumps by comparing changes in these averaged positions $|\Delta \bar{\mathbf{r}}_i|$ with the fluctuations in position $\sigma_{i,\text{est}}$ for each particle i where

$$|\Delta \bar{\mathbf{r}}_i| = |\bar{\mathbf{r}}_i(m) - \bar{\mathbf{r}}_i(m - 4 * 20)| \quad (6)$$

(see Fig. 1) and $\sigma_{i,\text{est}}$ is defined in [79]. We use in specific for $|\Delta \bar{\mathbf{r}}_i|$ not consecutive but instead average positions which are four averages (each of 20 configurations) apart. This choice of time interval in $|\Delta \bar{\mathbf{r}}_i|$ is to allow identification of not only sudden but also more gradual jumps. We define that a jump of particle i occurs whenever

$$|\Delta \bar{\mathbf{r}}_i|^2 > 20\sigma_{i,\text{est}}^2 \quad (7)$$

Notice that we use a relative criterion, namely for each particle i a comparison of $|\Delta \bar{\mathbf{r}}_i|$ with its $\sigma_{i,\text{est}}$. Our motivation for this relative criterion is that we would like to identify jumps of both A and the smaller B particles. Also even for particles of the same type their jump size might differ due to different cage sizes. $\sigma_{i,\text{est}}^2$ is an estimate for the cage size of each individual particle and is therefore used as criterion for the occurrence of a jump.

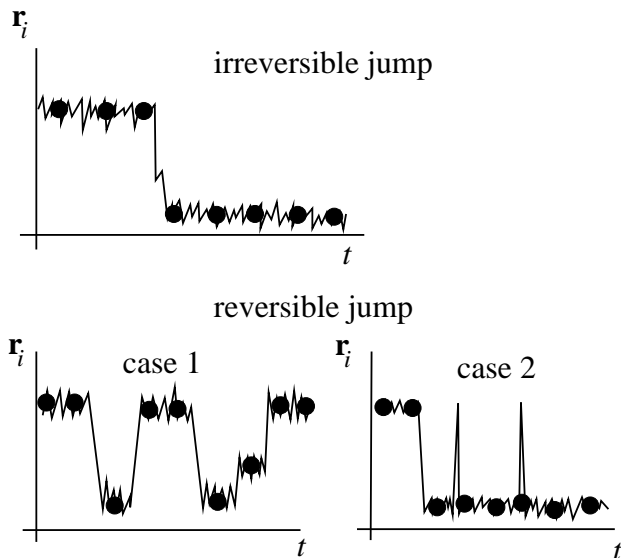


FIG. 2: Sketch of typical particle trajectories to illustrate the distinction between irreversible and reversible jumps

When we apply the above jump definition, we find two types of jumps which we call “irreversible” and “reversible” jumps (see Fig. 2). A particle which undergoes an irreversible jump succeeds in escaping its cage (for the time window of the simulation) whereas a particle undergoing a reversible jump returns back to one of its previous average positions. Similar results have been found in previous simulations of other systems [3, 4, 6, 8, 17, 21, 74]. However, the present work differs from these that we analyze all following quantities for the reversible and irreversible jumps separately. As sketched in Fig. 2, we call a jump reversible whenever case 1 or case 2 occurs. Case 1 corresponds to the situation of a particle undergoing multiple jumps and returning to one or more of any previous average positions (for details see Sec. V). If two average positions are equal then all jumps which happen between the previous position and the recurring position are called reversible jumps. In the example of Fig. 2 this means in case 1 that all shown jumps are reversible jumps. To increase our resolution in time we use not only the information of the averaged positions $\bar{\mathbf{r}}_i(m)$ but also the complete information of $\mathbf{r}_i(t)$. In case 2 (see Fig. 2) the spikes in $\mathbf{r}_i(t)$ indicate returns to the average position before the jump [80]. If a jump satisfies neither case 1 nor case 2, then it is called “irreversible jump.”

In the following we distinguish between the jump events, as they have been defined so far, and the corresponding jumping particles which may undergo multiple jumps of different types. Any reversible jump designates the corresponding particle as a reversible jumper for the entire time window.

IV. NUMBER OF JUMPING PARTICLES

We apply now the above definitions to identify all jumps occurring in our simulations. The number of identified jumps depends on the time interval of the production runs and, since the system is out of equilibrium, also on the waiting time before the production runs. The straightforward counting of jump events would give reversible jumpers (which sometimes jump many times) a larger weight. We therefore present the number of jumping particles. Fig. 3 shows the number of jumping particles normalized by the number N_α of particles in the system of type $\alpha \in \{A, B\}$. With increasing temperature T the number of jumping particles increases consistent with an increasing number of relaxation processes. A similar temperature dependence has been found indirectly via the participation ratio in the work [3, 48, 81]. More surprisingly, we find that not only the small B-particles are jumping but also a considerable fraction of A particles. However, the fraction of jumping B particles is larger than the fraction of jumping A particles due to the smaller size and therefore higher mobility of the B particles. Furthermore, both irreversible and reversible jumps are not only occurring in a certain temperature

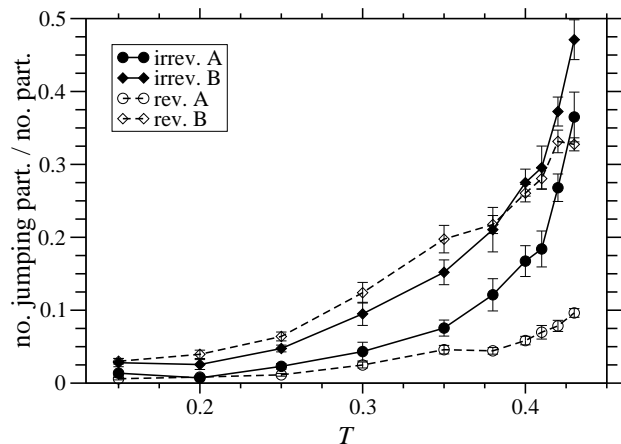


FIG. 3: Number of jumping particles normalized by the number of corresponding particle type as a function of temperature T . Irreversible and reversible jumpers are distinguished.

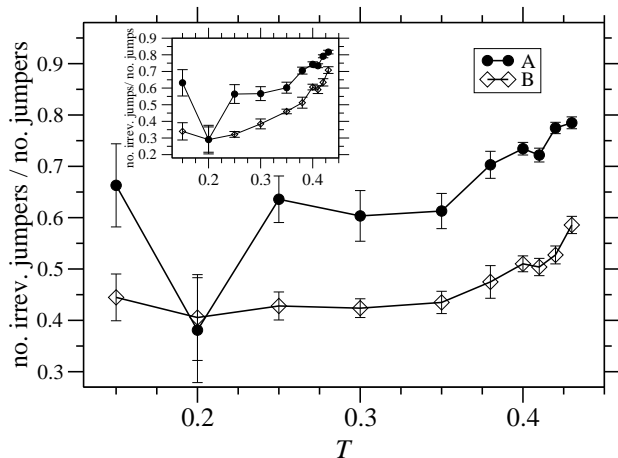


FIG. 4: Number of irreversible jumping particles divided by the number of both reversible and irreversible jumping particles. The inset shows the number of irreversible jump *events* divided by the number of jump *events*.

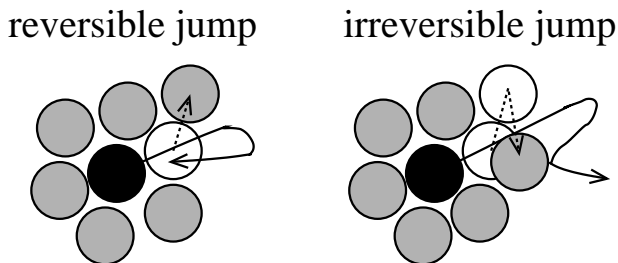


FIG. 5: This picture illustrates our interpretation of irreversible and reversible jumps and Fig. 4.

Fig. 4 illustrates the fraction of these jumping particles that are irreversible jumpers. At low to intermediate temperatures this ratio is, within the large error bars, roughly constant. At intermediate to larger temperatures irreversible jumpers become more likely than reversible jumpers with increasing temperature. This increase is even more pronounced for all temperatures if one considers the number of irreversible jump *events* (instead of jumping particles) divided by the number of all jump events (see inset of Fig. 4). Gaukel *et al.* [6, 8, 21] come to a similar conclusion via a model for their simulation data. Their irreversible jumps become more likely with increasing temperature. We interpret this increase in the fraction of irreversible jumps as sketched in Fig. 5. Both irreversible and reversible jumps start out the same, with the jumping particle leaving the cage (formed by the neighboring particles) possibly through an opening in the cage. In the case of the irreversible jump, the entrance of the cage gets meanwhile blocked by a particle, loosely speaking the door gets closed, and the jumping particle can no longer return and has successfully escaped its cage. With increasing temperature all particles become more mobile, which increases the likelihood of the blockage of the entrance back into the cage which in turn

leads to an increase in the fraction of irreversible jumps as shown in Fig. 4. We do not intend to make here a statement about the exact geometric process, for example that a door made up of a single particle gets open and closed, but more generally the process of rearrangement of the cage. Interestingly enough, this blockage happens more often in the case of the larger A than the smaller B-particles which leads to larger ratios for A than B-particles in Fig. 4.

V. NUMBER OF AVERAGE POSITIONS

With each jump a particle either returns to one of its former average positions within a cage or to a new overall average position. We call the average positions before and after a jump $\langle \bar{\mathbf{r}}_i \rangle_i$ and $\langle \bar{\mathbf{r}}_i \rangle_f$ (for details about the time averages $\langle \cdot \rangle_{i,f}$ see Fig. 11 and Sec. VII). We use as criterion for two average positions to be the same that the distance between them $\Delta \langle \bar{\mathbf{r}}_i \rangle = |\langle \bar{\mathbf{r}}_i \rangle_f - \langle \bar{\mathbf{r}}_i \rangle_i|$ and the average fluctuations before the jump $\langle \sigma_i^2 \rangle_i$ (for the defi-

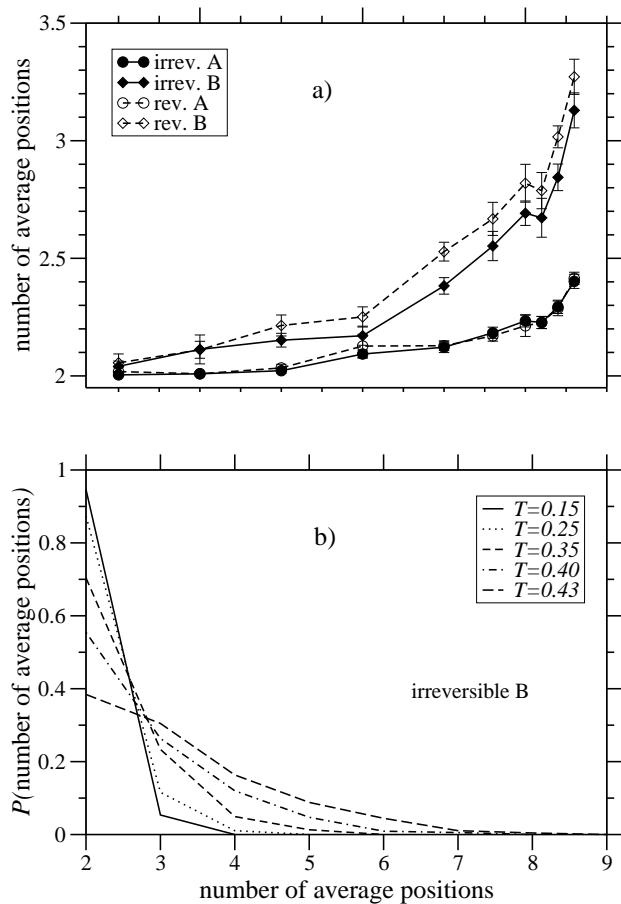


FIG. 6: The number of average positions (as defined in Sec. V) visited by jumping particles in a) as a function of temperature and in b) its distribution for irreversible jumping B particles.

shows an average of the number of distinct average positions which are visited by a particle. According to the higher mobility of the smaller B particles, they visit more average positions than the A particles. For low temperatures most jumping particles visit only two average positions during our simulation. For intermediate to larger temperatures, however, not only increasingly more particles jump (see Sec. IV) but these particles also jump more often. The distribution of the number of different visited average positions at the highest temperatures (as shown in Fig. 6b), broadens with increasing T such that some particles visit up to seven different average positions during the simulation run.

VI. TIMES

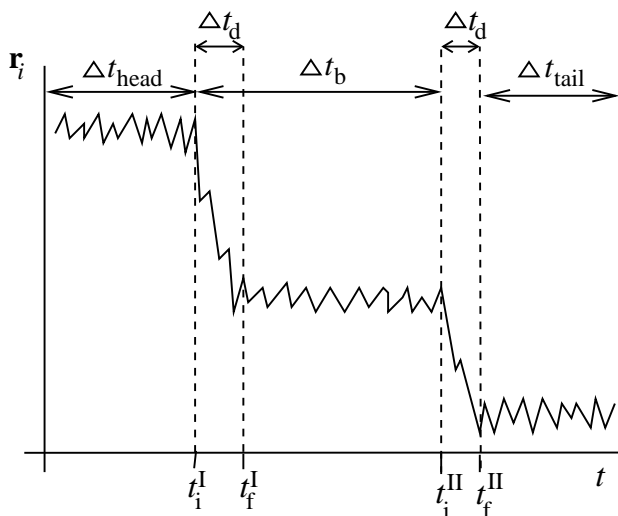


FIG. 7: Sketch to illustrate the definitions of the starting time t_i and ending time t_f of a jump (here for jumps I and II) and the times before the first jump of a particle Δt_{head} , during a jump Δt_d , between successive jumps Δt_b and after the last jump Δt_{tail} .

In this section we investigate the time scale of jumps. As sketched in Fig. 7 we determine the time duration of a jump $\Delta t_d = t_f - t_i$, the time before the first jump of a particle Δt_{head} , the time after the last jump of a particle Δt_{tail} , and the time between two successive jumps I and II to be $\Delta t_b = t_i^{II} - t_i^I$ where t_i and t_f indicate the starting and ending time of a jump [85]. Notice that Δt_b is only defined if a jump particle jumps twice or more and that we analyze Δt_{head} and Δt_{tail} separately as presented shortly. For the distinction of irreversible and reversible jumps, we assign the jump type of Δt_b according to the jump ending Δt_b , for example in Fig. 7 the jump type of Δt_b is determined by jump II. This means that Δt_b is a measure of the waiting time *before* a jump occurs. Fig. 8 illustrates that $\Delta t_d \ll \Delta t_b$ which tells us in hindsight why we could identify jumps as rare events with the above described procedure. Since the time resolution is

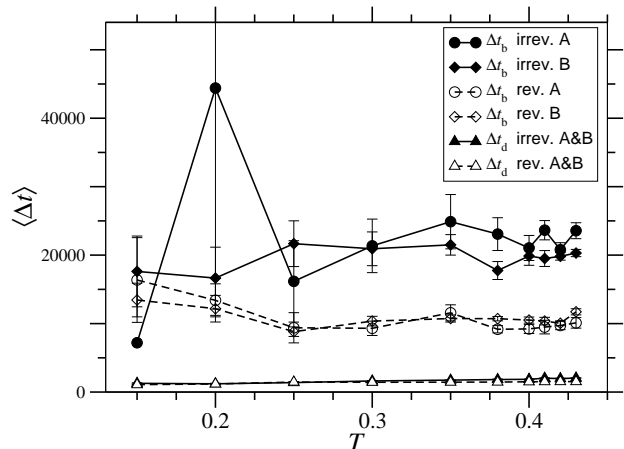


FIG. 8: Times between jumps Δt_b for A (circles) and B (diamonds) particles and times during jumps Δt_d for both A and B particles.

of the order of 1000 ($\approx 20 \cdot 2000 \cdot 0.02$), i.e. of the same order as Δt_d , we do not draw further conclusions about the temperature dependence of Δt_d . However, Δt_b is well above our time resolution and small enough to be detected during our simulation run of length $1 \cdot 10^5$. In accordance with the picture of reversible jumpers which try but do not succeed to escape their cage, these trials happen on a shorter time scale than irreversible jumps. However, to our surprise, Δt_b seems to be independent not only of the particle type but also of temperature. The question arises if this temperature independence of Δt_b is a consequence of the finite time window of our simulation. To take this finite time interval t_{tot} into account, we make a crude approximation to correct the time intervals Δt_b , Δt_{head} and Δt_{tail} by assuming that jumps happen equally likely at any time in the window $[0, t_{\text{tot}}]$ (which is not accurate due to aging). The probability $P_{\text{corr}}(\Delta t)$ of finding the complete interval Δt reduces to the probability of finding Δt during $[0, t_{\text{tot}}]$ in the simulation

$$P_{\text{sim}}(\Delta t) = P_{\text{corr}}(\Delta t) \cdot \frac{(t_{\text{tot}} - \Delta t)}{t_{\text{tot}}} \cdot c \quad (8)$$

where c is a normalization constant. We may approximate c with $\left\langle \frac{t_{\text{tot}}}{t_{\text{tot}} - \Delta t} \right\rangle_{\text{sim}}^{-1}$ where $\langle \cdot \rangle_{\text{sim}}$ indicates an average over jump events of the simulation. We thus obtain

$$P_{\text{corr}}(\Delta t) \approx \frac{P_{\text{sim}}(\Delta t)}{(t_{\text{tot}} - \Delta t)} \cdot \left\langle \frac{1}{(t_{\text{tot}} - \Delta t)} \right\rangle_{\text{sim}}^{-1} \quad (9)$$

Similarly the average times $\langle \Delta t \rangle_{\text{sim}}$ may be approximately corrected by

$$\langle \Delta t \rangle_{\text{corr}} \approx \left\langle \frac{\Delta t}{(t_{\text{tot}} - \Delta t)} \right\rangle_{\text{sim}} \cdot \left\langle \frac{1}{(t_{\text{tot}} - \Delta t)} \right\rangle_{\text{sim}}^{-1} \quad (10)$$

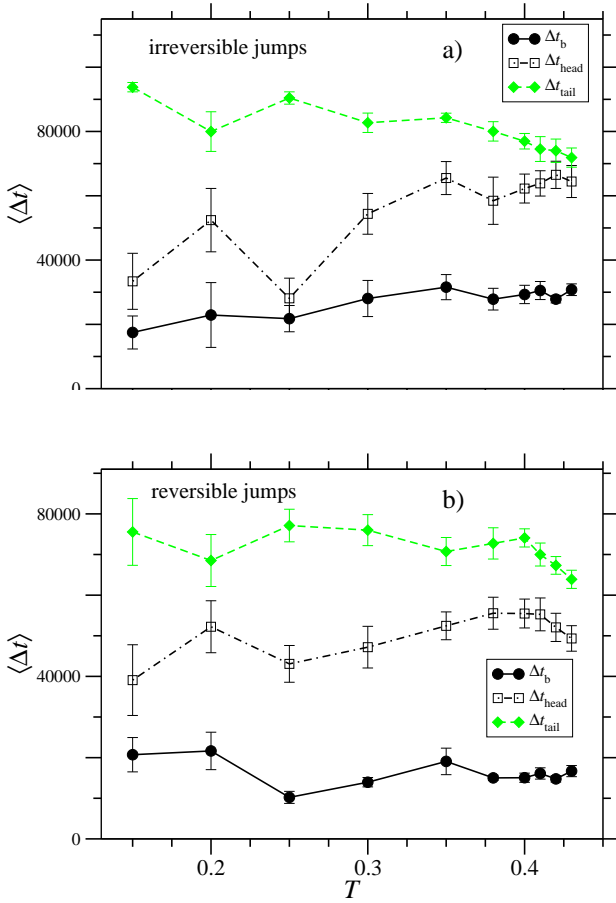


FIG. 9: Times Δt_b , Δt_{head} and Δt_{tail} a) for irreversible jumps and b) for reversible jumps of A and B particles using Eq. (10).

Fig. 9a and Fig. 9b show the resulting corrected times $\langle \Delta t \rangle_{\text{corr}}$ for irreversible and reversible jumps respectively. For simplification of notation we drop $\langle \cdot \rangle_{\text{corr}}$ in the following. The tail and head times, Δt_{tail} and Δt_{head} , reveal that we find aging, since $\Delta t_{\text{tail}} > \Delta t_{\text{head}}$, i.e. jumps are more likely to occur at the beginning of the simulation than later. This particular aging effect decreases with increasing temperature. Δt_{tail} and Δt_{head} are both larger than Δt_b because Δt_b includes only times of particles which jump multiple times whereas Δt_{head} and Δt_{tail} include also times of particles which jump only once. Interestingly, Δt_b is (although approximately corrected) still independent of temperature. Together with our results of Secs. III – V we therefore find that with increasing temperature relaxation processes are accelerated via more jumping particles and more multiple jumps, but the times between multiple jumps do not become shorter. This is contrary to previous results [19, 34, 58, 59, 82] in which waiting times decrease with increasing temperature. In our system, however, the temperature independence seems to be true not only for the averages but even for the distribution $P_{\text{corr}}(\Delta t_b)$ (see Fig. 10). We interpret this temperature independence as being due to aging

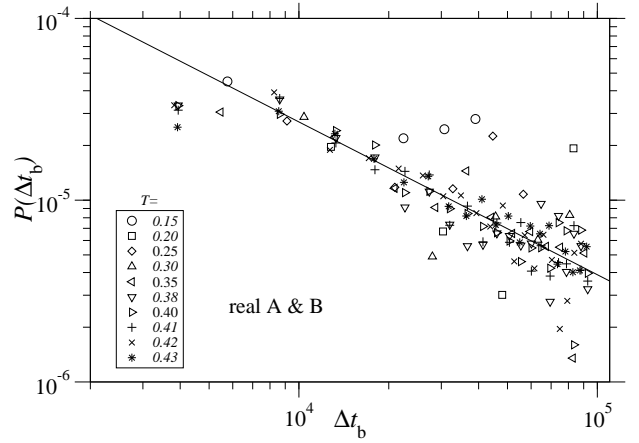


FIG. 10: Log-log plot of $P(\Delta t_b)$ using Eq. (9) for irreversible jumps of A and B particles. The line is a linear fit to the data with slope -0.84 .

which is consistent with our data for Δt_{tail} and Δt_{head} and with the results of Doliwa *et al.* [58, 59] who find that the distribution of waiting times initially is temperature independent and becomes temperature dependent at later times. As shown in Fig. 10 for irreversible jumps of A and B particles, $P(\Delta t_b)$ approximately follows a power law $P(\Delta t_b) \propto \Delta t_b^{-\nu}$ with $\nu = 0.84$. Even though we expect the system to show normal diffusion on a time scale much larger than our simulation run, the intermediate dynamics is subdiffusive [83]. Please notice however that a direct comparison of our result with the scheme presented in Fig. 1 of [83] is not possible because in our case the multiple jumps of one particle at different times as well as the jumps of different particles are not independent, which changes the dynamics [84].

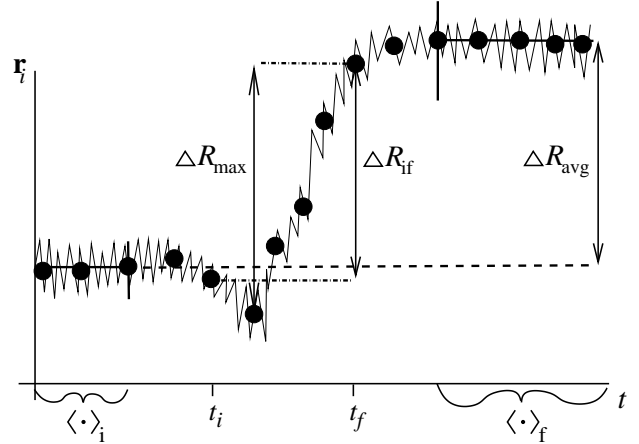


FIG. 11: Sketch for the definitions of ΔR_{if} , ΔR_{max} and ΔR_{avg} .

VII. JUMP LENGTHS

In the last sections we have investigated how many particles jump and how often jumps occur. Next we study how far these particles jump. To be able to test if our qualitative results are dependent on the definition of jump length, we use three quantities: ΔR_{if} , ΔR_{max} and ΔR_{avg} as sketched in Fig. 11. For a jump of particle i the jump distance of the jump starting at t_i and ending at t_f (for the definition of t_i and t_f see [85]) is

$$\Delta R_{\text{if}} = |\bar{\mathbf{r}}_i(t_i) - \bar{\mathbf{r}}_i(t_f)| \quad (11)$$

and the maximal distance being detected during the jump

$$\Delta R_{\text{max}} = \max_t |\bar{\mathbf{r}}_i(t) - \bar{\mathbf{r}}_i(t - 3200)| \quad (12)$$

(here $3200 = 4 \cdot 20 \cdot 2000 \cdot 0.02$ as in [79] and Sec. III) where t is varied over times t which satisfy $t_{i,\text{detect}} \leq t < t_{f,\text{detect}}$ ([85]). The third length ΔR_{avg} is less dependent on fluctuations than ΔR_{if} and ΔR_{max} . It is the distance of the overall average positions before and after the jump

$$\Delta R_{\text{avg}} = |\langle \bar{\mathbf{r}}_i \rangle_f - \langle \bar{\mathbf{r}}_i \rangle_i| \quad (13)$$

For the averages $\langle \cdot \rangle_f$ and $\langle \cdot \rangle_i$ the positions $\bar{\mathbf{r}}_i(t)$ are averaged over times before and after the jump excluding a broadened time window around the jump $[t_i - 800, t_f + 800]$. Fig. 12a shows that the different jump lengths have the same qualitative behavior, namely, as one might expect, an increase with increasing temperature T . We therefore show in the following mainly results for only ΔR_{avg} but find very similar behavior in the case of ΔR_{if} and ΔR_{max} . An increase in jump size with increasing temperature has been seen in previous simulations [3, 19, 34, 48, 81]. However in the case of [3, 48, 81] the jump size is for a jump in the MSD, i.e. an average over all particles, which includes two effects: an increasing number of jumping particles and an increase in the jump size of single particle jumps. Our approach has the advantage of keeping these two effects separate. Furthermore, in our case the single particle jumps are larger than in [3, 34, 48, 81].

Fig. 12b is the same as Fig. 12a for ΔR_{avg} but broken down by both jump and particle type. The smaller B particles are jumping further than the A particles. Furthermore reversible jumps are shorter than the irreversible jumps, which is due to two features in the distribution $P(\Delta R_{\text{avg}})$.

As illustrated in Fig. 13 both irreversible and reversible jumps have a peak at about 0.8 and 1.0 for A and B particles respectively. These peaks are relatively similar for reversible and irreversible jumps, taking aside that for irreversible jumps this peak position is slightly shifted to the right and slightly broadened (partly due to multiple jumps which are not resolved in time). This similarity and the peak positions around unity are consistent with our picture that irreversible and reversible jumps start out the same, namely with a particle jumping out of its

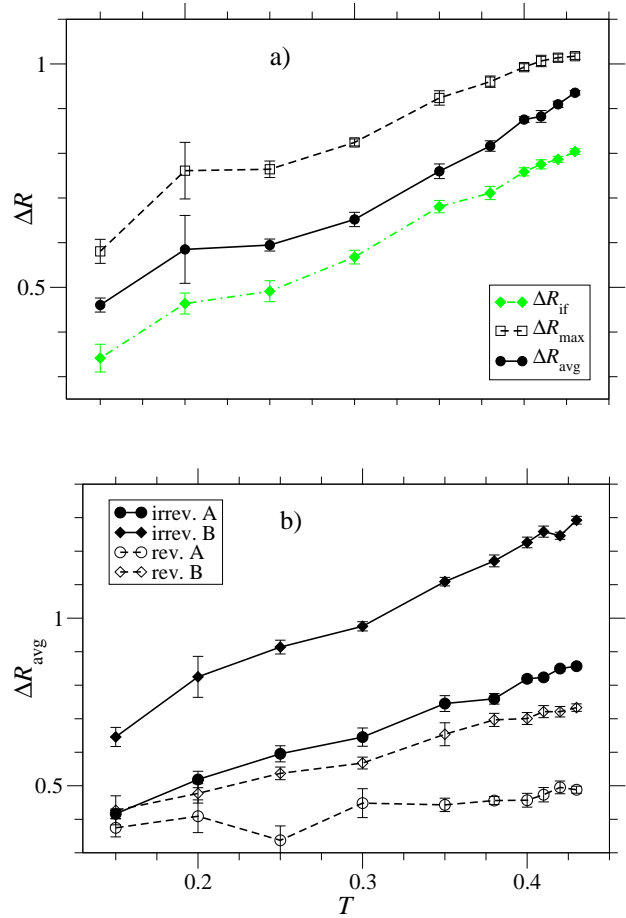


FIG. 12: a) The jump sizes ΔR_{if} , ΔR_{max} and ΔR_{avg} (sketched in Fig. 11 and defined in the text) as function of temperature T . The averages are over both irreversible and reversible jumps of both A and B particles. b) The jump size ΔR_{avg} as function of temperature T separately for irreversible and reversible jumps of A and B particles.

cage. A new feature, however, is that the distribution of reversible jumps for $T = 0.43$ (and similarly for all other temperatures) has a bimodal distribution with an additional peak at a distance smaller than 0.2, contrary to the distribution of irreversible jumps. This seems to indicate for reversible jumps another process than a jump out of a cage because the latter would be of the order 0.5 and larger.

The increase of ΔR_{avg} with increasing temperature is a consequence of both a shift of the peak position and a broadening of the distribution of jump sizes. This is illustrated in the inset of Fig. 13 for irreversible jumps of A particles and we find similar distributions for irreversible jumps of B particles. At the largest investigated temperature $T = 0.43$ some of the particles move as far as four particle spacings. Some of these large jumps might correspond to multiple jumps of a smaller time window than our time resolution.

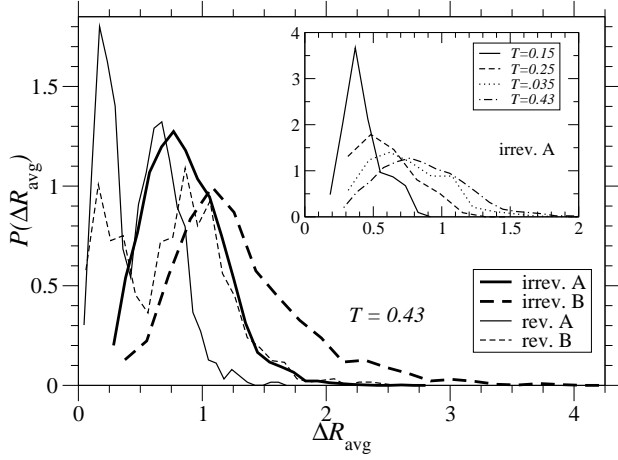


FIG. 13: The distribution of jump sizes ΔR_{avg} for irreversible and reversible jumps of A and B particles at $T = 0.43$. The inset shows ΔR_{avg} of irreversible jumping A particles for different temperatures.

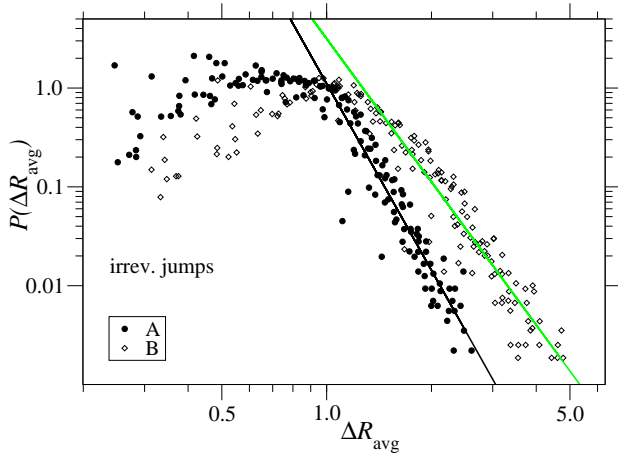


FIG. 14: Log-log plot of the distribution of jump sizes ΔR_{avg} for irreversible jumps of A and B particles including all temperatures. The lines are linear fits with slopes -6.3 for A and -4.8 for B particles.

For irreversible jumps of size unity and larger we find that the distribution for all temperatures follow roughly a power law $P(\Delta R) \approx \Delta R^{-\mu}$ (see Fig. 14) with $\mu = 6.3$ for A and $\mu = 4.8$ for B particles. This is in accordance with subdiffusive behavior for intermediate times as presented in Sec. VI for the distribution of waiting times [83].

As commented on earlier (see Sec. I and Sec III), our definition for a jump is not based on a specified size but instead a multiple of the fluctuations of the particle. Let us therefore next look at the fluctuations. Fig. 15 shows a comparison of the fluctuations of jumping particles σ_{jump} and of non-jumping particles σ_{nojump} . Also included in Fig. 15 is an average over all particles σ_{est} of the estimates for fluctuations $\sigma_{i,\text{est}}$ as they have been used for the jump

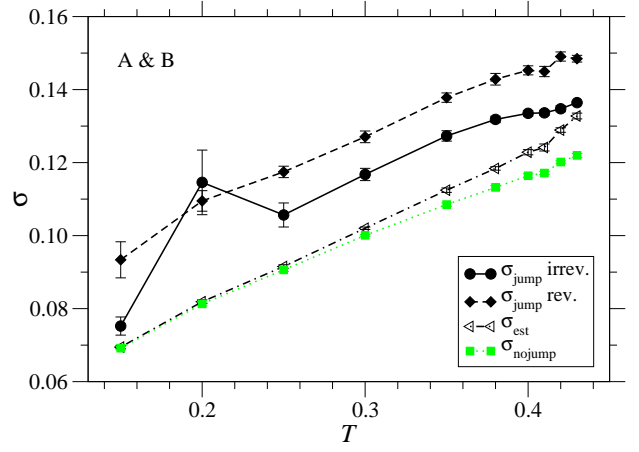


FIG. 15: Fluctuations in position σ for jumping particles σ_{jump} , of the original estimate for jumping particles σ_{est} , and for non-jumping particles σ_{nojump} . For the average of σ_{jump} fluctuations during the jump have been excluded from the average.

identification (see Sec. III and [79]). σ_{est} is very similar to σ_{nojump} and represents the fluctuations of an average particle. For the average of σ_{jump} we exclude fluctuations during the jump: for jumping particle i we take

$$\sigma_{i,\text{jump}} = \left(\frac{\langle \sigma_i^2 \rangle_f + \langle \sigma_i^2 \rangle_i}{2} \right)^{1/2} \quad (14)$$

where σ_i and $\langle \cdot \rangle_{i,f}$ are defined as in [79] and earlier in this section respectively. Although jump times are excluded, the fluctuations of jumping particles are clearly larger than the fluctuations of non-jumping particles. This means that jumping particles are not only moving farther than an average particle during single events but are also oscillating within their cages with a larger than average amplitude.

Fig. 16a shows an average of jump size relative to the particle's fluctuation $\Delta R_{i,\text{avg}}/\sigma_{i,\text{jump}}$ for jumping particles i . $\Delta R_{\text{avg}}/\sigma_{\text{jump}}$ seems independent of temperature for reversible jumps and for irreversible jumps slightly increasing with increasing temperature.

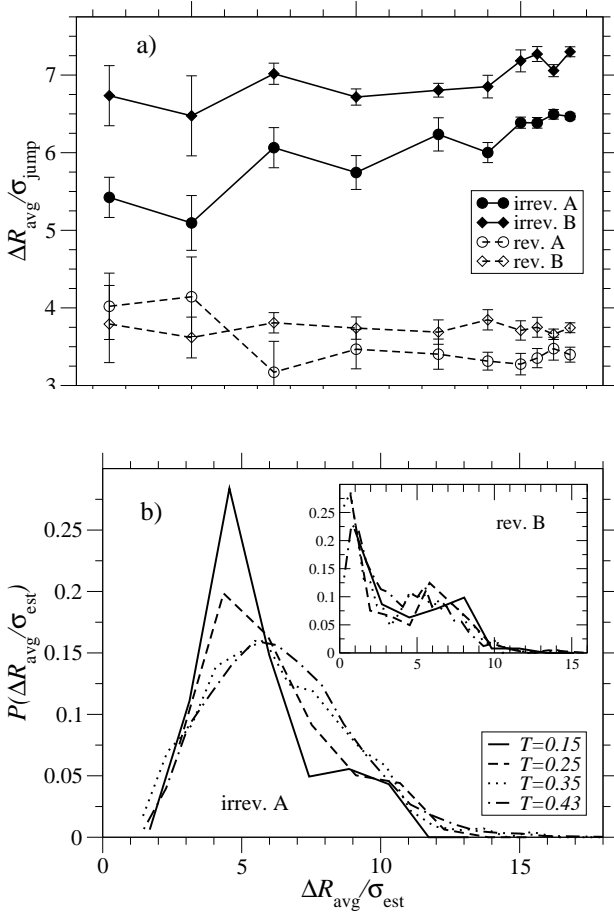


FIG. 16: a) Normalized jump size $\Delta R_{\text{avg}}/\sigma_{\text{jump}}$ as function of temperature separately for irreversible and reversible jumps of A and B particles. b) Distribution of normalized jump size $P(\Delta R_{\text{avg}}/\sigma_{\text{est}})$ of irreversible jumping A particles and reversible jumping B particles in the inset.

The distribution of $\Delta R/\sigma$ gives us the opportunity to estimate the influence of the cutoff in our definition of a jump. Similar to our approach for the search of a jump, we use σ_{est} , and obtain $P(\Delta R_{\text{avg}}/\sigma_{\text{est}})$ as shown in Fig. 16b for irreversible jumps of A particles. We find a peak at $(\Delta R_{\text{avg}}/\sigma_{\text{est}}) \approx 5.5$ (for B-particles ≈ 6.5), i.e. larger than our cutoff at $(\Delta R/\sigma) = \sqrt{20} \approx 4.5$. This gives us the hope that we have included the major contribution of jumps consistent with our approach. We have to bear in mind, however, that $\Delta R_{\text{avg}}/\sigma_{\text{est}}$ is not the identical measure to the one used in our search procedure. Furthermore, in the case of reversible jumps there is some additional peak at smaller values of $(\Delta R_{\text{avg}}/\sigma_{\text{est}})$ (see inset of Fig. 16b) which is consistent with Fig. 13 and might indicate some additional process.

VIII. ENERGY

In the previous sections we have investigated relaxation processes by solely using the positions (trajectories) of

single particles. As the work [55, 56, 57, 58, 59, 60] shows, an approach via potential energies can also be fruitful. We therefore study in this section what happens to the potential energy during jumps. As sketched in

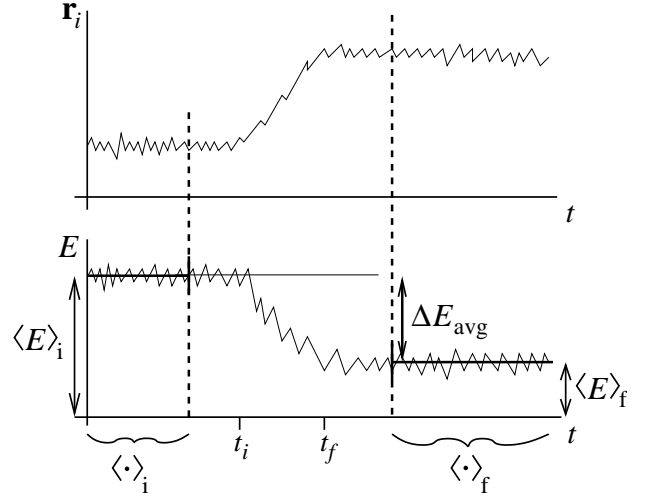


FIG. 17: Sketch for the definitions of $\langle E \rangle_i$ and $\langle E \rangle_f$.

Fig. 17, we still use single particle trajectories to identify the jumping particle and do similar averaging for the according time windows $\langle \cdot \rangle_i$ and $\langle \cdot \rangle_f$ (see Sec. VII). We investigate both the total potential energy per particle

$$E(t) = \frac{1}{N} \sum_{i=1}^N \sum_{j>i} V_{\alpha\beta}(r_{ij}(t)) \quad (15)$$

and the single particle potential energy of particle i

$$E_i(t) = \sum_{j \neq i} V_{\alpha\beta}(r_{ij}(t)) \quad (16)$$

where $V_{\alpha\beta}(r_{ij}(t))$ is defined in Eq. (5). To obtain in addition the energies of the inherent structures [86] we minimized the configurations $(\{\mathbf{r}_i(t)\})$ via a steepest descent procedure. With the thus obtained configuration $(\{\mathbf{r}_i^0(t)\})$ we determine

$$E^0(t) = \frac{1}{N} \sum_{i=1}^N \sum_{j>i} V_{\alpha\beta}(r_{ij}^0(t)) \quad (17)$$

and

$$E_i^0(t) = \sum_{j \neq i} V_{\alpha\beta}(r_{ij}^0(t)) \quad (18)$$

Similar to the jump size in position (see Fig. 17 and Sec. VII) we then determine

$$\Delta E_{\text{avg}} = \langle E(t) \rangle_f - \langle E(t) \rangle_i \quad (19)$$

and

$$\Delta E_{if} = E(t_f) - E(t_i) \quad (20)$$

and similarly for the energies of Eq. (16) – (18).

We find in most of our analysis that ΔE_{avg} and ΔE_{if} (and all other equivalents for E^0 , E_i and E_i^0) are showing the same qualitative behavior, and therefore present in the following results for ΔE_{avg} using Eq. (19) and

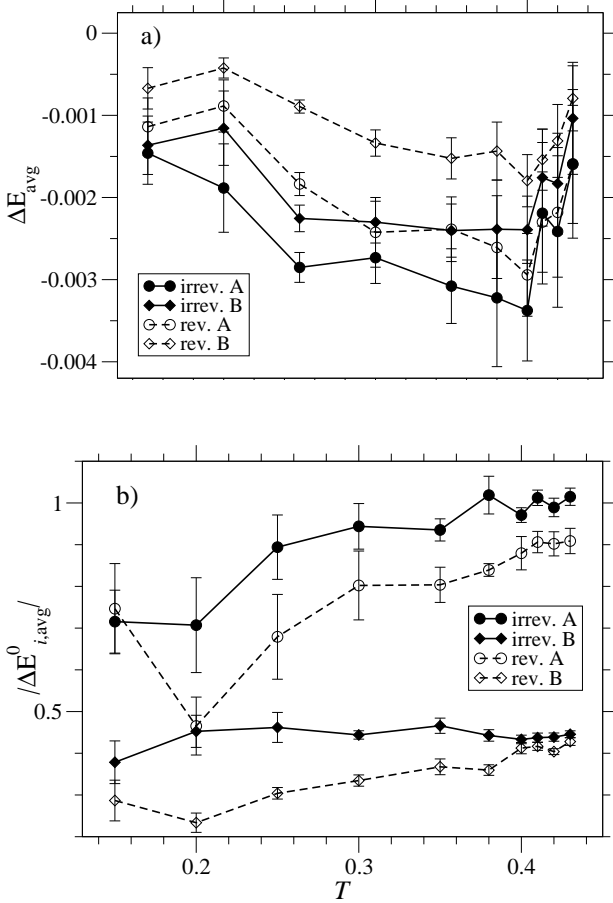


FIG. 18: As a function of temperature T a) jump size in total potential energy ΔE_{avg} and b) absolute value of the jump size in minimized single particle potential energy $|\Delta E_{i,\text{avg}}^0|$.

Fig. 18a shows ΔE_{avg} as a function of temperature averaged separately over irreversible and reversible jumps of A and B particles. Notice that the energy jumps are small compared to energy values $\langle E \rangle_{i,f} \approx -7$. The irreversible jumps lower the energies more than reversible jumps and more so for A than B particles, because a jump of a larger A particle results in a bigger change in environment than for a smaller B-particle. The lowering of the total potential energy happens mostly at intermediate temperatures and less at the lowest and highest investigated temperatures. This might be an aging effect: at low temperatures the system is basically frozen in, at intermediate temperatures the system has time to partially age, and at higher temperatures the system has already aged before the production run starts. This effect is lost when we look at the jumps in single particle

energies $\Delta E_{i,\text{avg}}(T)$ which is basically zero for all jumps. We therefore find that the total potential energies ΔE_{avg} , ΔE_{if} , ΔE_{avg}^0 , and ΔE_{if}^0 show a more systematic dependence on temperature than their single particle equivalents $\Delta E_{i,\text{avg}}$ etc.. For the absolute values $|\Delta E_{\text{avg}}|$ etc. and all following quantities, however, we find the opposite, i.e. the single particle equivalents $|\Delta E_{i,\text{avg}}|$ etc. show a more pronounced behavior. We therefore show from now on the results which use Eq. (16) and Eq. (18) only.

We next look at the absolute value $|\Delta E_{i,\text{avg}}^0|$ as a function of temperature (see Fig. 18b). As one might expect, the irreversible jumps show larger changes in energy than reversible jumps, due to larger jumps in position (Fig. 12b) and therefore more change in the environment of the jumping particle. And similarly the larger A particles in comparison with the smaller B particles experience a larger change in energy because A particles are surrounded by more neighbors, i.e. a larger environment. With increasing temperature the absolute value of the jump in energy (Fig. 18b) is increasing (with the one exception of irreversible B particles) which is consistent with the increase in jump position (Fig. 12b).

We define the fluctuations in energy σ_{E_i} at time $t = m \cdot 2000 \cdot 0.02$

$$\sigma_{E_i} = \left(\frac{1}{2} \left\langle \left\langle \frac{1}{20} \sum_{m'=m-9}^{m+10} (E_i(m') - \bar{E}_i(m'))^2 \right\rangle_i + \left\langle \frac{1}{20} \sum_{m'=m-9}^{m+10} (E_i(m') - \bar{E}_i(m'))^2 \right\rangle_f \right\rangle \right)^{-1/2} \quad (21)$$

similar to the fluctuations in position [79] where $\bar{E}_i(m)$ is the time average $\frac{1}{20} \sum_{m'=m-9}^{m+10} E_i(m')$. The energy fluctuations are also increasing with increasing temperature and are larger for A than B particles (see Fig. 19a). The fluctuations of irreversible and reversible jumps are however very similar, which is consistent with the picture that reversible jumps are “failed” irreversible jumps and in that sense start out the same way as irreversible jumps.

Fig. 19b is a comparison of energy fluctuations of jumping (both irreversible and reversible and of both A and B) particles $\sigma_{E_{i,\text{jump}}}$ and of non-jumping particles $\sigma_{E_{i,\text{nojump}}}$ [87]. In $\sigma_{E_{i,\text{jump}}}$ we exclude the times during the jump by using the time windows $\langle \cdot \rangle_{i,f}$. We find that the energy fluctuations of jumping particles are larger than for non-jumping particles which is consistent with the corresponding fluctuations in position (see Fig. 15).

By normalizing $|\Delta E_{i,\text{avg}}|$ with the fluctuations σ_{E_i} we obtain Fig. 20a. Similar to the case of normalized jumps in position (Fig. 16a) we find that $|\Delta E_{i,\text{avg}}|/\sigma_{E_i}$ is for reversible jumps basically independent of temperature. For irreversible jumps, however $|\Delta E_{i,\text{avg}}|/\sigma_{E_i}$ decreases significantly with increasing temperature. This indicates that with increasing temperature the jumps are increasingly more driven by fluctuations. Contrary to the equivalent in position (Fig. 16a), the normalized energies are significantly smaller, in the range 0.5 – 1.4 rather than 3 – 7, and the distribution of $|\Delta E_{i,\text{avg}}|/\sigma_{E_i}$ (see Fig. 20b) is monotonous decreasing with a less far reaching tail than

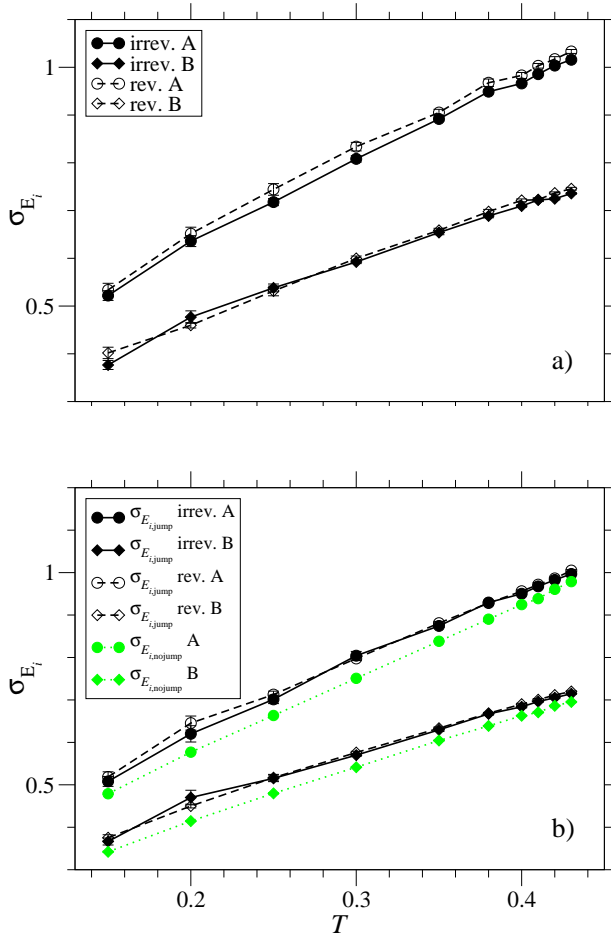


FIG. 19: Fluctuations in single particle potential energy as a function of temperature. The average is in a) over irreversible and reversible jump *events* of A and B particles separately and in b) over jumping *particles* ($\sigma_{E_{i,\text{jump}}}$) and over non-jumping *particles* ($\sigma_{E_{i,\text{nonjump}}}$).

IX. CONCLUSIONS

We study the dynamics of a binary Lennard-Jones system below the glass transition. Our focus is on jump-

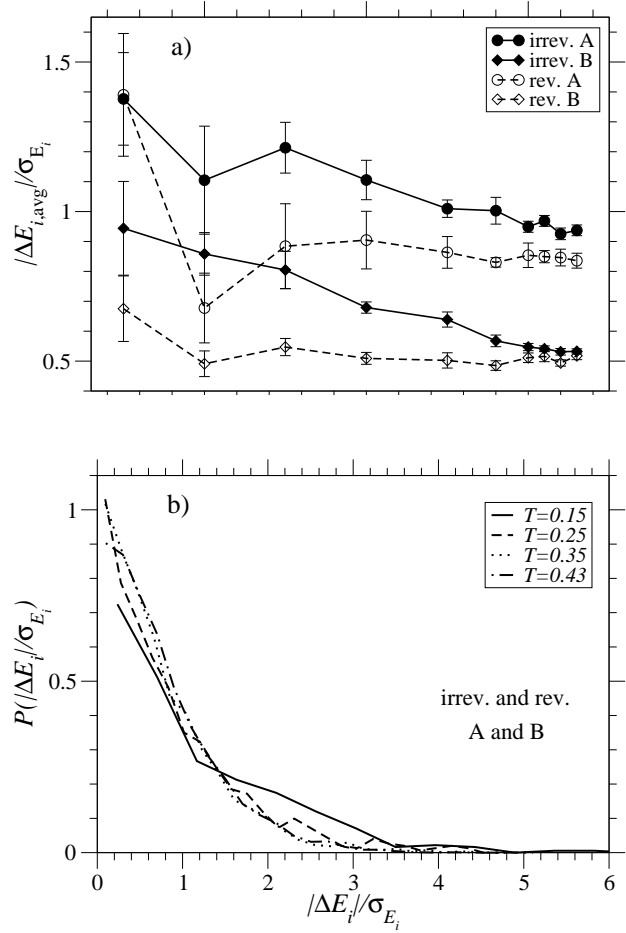


FIG. 20: Absolute value of single particle potential energy divided by its fluctuation $|\Delta E_{i,\text{avg}}|/\sigma_{E_i}$ in a) as a function of temperature and in b) its distribution .

processes, which we identify via single particle trajectories. Two kind of jumps are found: “reversible jumps,” where a particle jumps back and forth between one or more average positions, and “irreversible jumps,” where a particle does not return to any of its former average positions, i.e. successfully escapes its cage of neighbors. Both irreversible and reversible jumps of A and B particles occur at all temperatures. With increasing temperature more particles jump, more average positions are visited, the jump size both in position and in the absolute value of the potential energies $|\Delta E|$, $|\Delta E^0|$, $|\Delta E_i|$ and $|\Delta E_i^0|$ (total and single-particle, not minimized and minimized) increase, and the fluctuations in position σ_R and potential energy σ_E increase. The fluctuations are larger for jumping particles than for non-jumping particles even if fluctuations during the jump are not part of the average, which indicates that jumping particles are not only during jump times more mobile than non-jumping particles. The ratio $|\Delta E_i|/\sigma_{E_i}$ of irreversible jumps decreases with increasing temperature. This confirms a commonly used assumption that with increasing temperature the irreversible jumps become more driven

by fluctuations.

With increasing temperature also irreversible jumps become proportionally more frequent than reversible jumps. We interpret this such that irreversible and reversible jumps are similar in that sense that a particle tries to escape its cage. In the case of reversible jumps the particle finds its way back into the cage whereas in the case of an irreversible jump the path back into the cage becomes blocked due to rearrangements of the cage. At larger temperature these rearrangements of the cage become more likely (since for example the fluctuations increase) and therefore irreversible jumps occur more often. Irreversible and reversible jumps show in most quantities qualitatively the same behavior, such as their temperature dependence of jump size in position and energy, and differ only in size. An exception to this similarity is the distribution of jump sizes, which suggests that there might be an additional jump process in the case of reversible jumps indicated by an additional peak at small jump sizes.

The most surprising result of our work is that the times between successive jumps are independent of temperature. This is most likely due to aging, which could mean on the time scale of our simulation that Δt_b reflects the time scale of $T = 0.446$ from which we quenched the system, and that Δt_b might show temperature dependence at later times. The latter would be consistent with the work of Doliwa *et al.* [58, 59] who find in their simulations of very long times that the distribution of waiting times (however, identified via the collective quantity of the minimized potential energy) initially is temperature independent and of different power law than at later times when temperature dependence occurs. We do find aging in that sense that the times before the first jump are shorter than the times after the last jump of a particle (an effect which becomes less for temperatures near T_c).

Future work (which is in progress) will tell us if in our system Δt_b becomes temperature dependent after longer times. However, the dynamics does depend on temperature for all other here investigated quantities such as the number of jumps and the fraction of reversible jumps.

Another question which we would like to raise for future work is how much single particle jumps can tell us about relaxations of a glass which might include collective motion. It seems plausible that single particle jumps are strongly correlated with collective jumps and in that sense give us very similar information to studies of collective quantities. We find that many of the single particle jumps in our system are spatially and temporally correlated, i.e. are showing collective motion. Systematic studies for confirmation remain to be done in the future. We also find the signature of many-particle effects confirmed in the result of the increasing ratio of irreversible jumps with increasing temperature, since this indicates that not only the jumping particle itself but also its cage are dependent on temperature. There might, however, be also collective jumps, where each particle jumps a too small amount to be detected by our search algorithm. It remains to be studied of how much importance such processes are in our system.

Acknowledgments

I would like to thank K. Binder and A. Zippelius for hospitality, financial support and for their helpful discussions. I also thank J. Horbach for helpful discussions and B. Vollmayr-Lee and J. Horbach for the careful reading of this manuscript. I gratefully acknowledge financial support from SFB 262 and DFG Grant No. Zi 209/6-1.

-
- [1] For reviews see e.g. R. Zallen, *The Physics of Amorphous Materials* (Wiley, New York, 1983); J. Jäckle, Rep. Prog. Phys. **49**, 171 (1986); W. Götze and L. Sjögren, Rep. Prog. Phys. **55**, 241 (1992); C. A. Angell, Science **267**, 1924 (1995); Proceedings of 3rd International Discussion Meeting on Relaxation in Complex Systems Ed.: K. L. Ngai, J. Non-Cryst. Solids **235-238** (1998).
 - [2] Examples of the mean square displacement as a function of time (logarithmically plotted) are given in W. Kob and H. C. Andersen, Phys. Rev. E **51**, 4626 (1995).
 - [3] C. Oligschleger, C. Gaukel and H. R. Schober, J. Non-Cryst. Solids **250-252**, 660 (1999); C. Oligschleger and H. R. Schober, Phys. Rev. B **59**, 811 (1999).
 - [4] H. Teichler, J. Non-Cryst. Solids **293-295**, 339 (2001); H. Teichler, J. Non-Cryst. Solids **312-314**, 533 (2002).
 - [5] H. R. Schober, J. Non-Cryst. Solids **307**, 40 (2002).
 - [6] C. Gaukel, M. Kluge and H. R. Schober, Phil. Mag. B **79**, 1907 (1999).
 - [7] D. Caprion and H. R. Schober, Phys. Rev. B **62**, 3709 (2000).
 - [8] H. R. Schober, C. Gaukel, and C. Oligschleger, Defect and Diffusion Forum **143**, 723 (1997).
 - [9] S. Sanyal and A. K. Sood, Phys. Rev. E **52**, 4154 (1995).
 - [10] J. M. Delaye and Y. Limoge, J. Phys. I **3**, 2063 (1993).
 - [11] N. Lačević, F. W. Starr, T. B. Schröder, V. N. Novikov, and S. C. Glotzer, Phys. Rev. E **66**, 030101(R) (2002); S. C. Glotzer, V. N. Novikov, and T. B. Schröder, J. Chem. Phys. **112**, 509 (2000).
 - [12] S. C. Glotzer, Y. Gebremichael, N. Lačević, T. B. Schröder, and F. W. Starr, ACS Sym. Ser. **820**, 214 (2002).
 - [13] B. Doliwa and A. Heuer, J. Phys.:Condens. Matter **11**, A277 (1999).
 - [14] B. Doliwa and A. Heuer, Phys. Rev. Lett. **80**, 4915 (1998).
 - [15] R.-J. Roe, J. Chem. Phys. **100**, 1610 (1994).
 - [16] S. Sanyal and A. K. Sood, Europhys. Lett. **34**, 361 (1996).
 - [17] G. Wahnström, Phys. Rev. A **44**, 3752 (1991).
 - [18] S. Bhattacharyya, A. Mukherjee, and B. Bagchi, J.

- Chem. Phys. **117**, 2741 (2002).
- [19] M. Kluge, Ph.D. thesis, Berichte des Forschungszentrums Jülich **3913**, Jülich, Germany (2001).
- [20] C. Gaukel and H. R. Schober, Sol. State Commun. **107**, 1 (1998).
- [21] C. Gaukel, M. Kluge and H. R. Schober, J. Non-Cryst. Solids **250-252**, 664 (1999).
- [22] T. B. Schröder, J. C. Dyre, J. Non-Cryst. Solids **235-237**, 331 (1998).
- [23] J. N. Roux, J. L. Barrat and J.-P. Hansen, J. Phys.:Condens. Matter **1**, 7171 (1989).
- [24] R. Brüning, D. H. Ryan, J. O. Ström-Olsen, and L. J. Lewis, Material Science and Engineering **A134**, 964 (1991).
- [25] W. Kob, C. Donati, S. J. Plimpton, P. H. Poole and S. C. Glotzer, Phys. Rev. Lett. **79**, 2827 (1997)
- [26] C. Donati, J. F. Douglas, W. Kob, S.J. Plimpton, P.H. Poole and S.C. Glotzer, Phys. Rev. Lett. **80**, 2338 (1998); C. Donati, S. C. Glotzer, P. H. Poole, W. Kob and S. J. Plimpton, Phys. Rev. E **60**, 3107 (1999).
- [27] R. Yamamoto and A. Onuki, Phys. Rev. Lett. **81**, 4915 (1998).
- [28] W. K. Kegel and A. van Blaaderen, Science **287**, 290 (2000).
- [29] E. R. Weeks, J. C. Crocker, A. C. Levitt, A. Schofield, and D. A. Weitz, Science **287**, 627 (2000).
- [30] E. R. Weeks and D. A. Weitz, Phys. Rev. Lett. **89**, 095704 (2002).
- [31] M. M. Hurley and P. Harrowell, J. Chem. Phys. **105**, 10521 (1996).
- [32] D. Caprion, J. Matsui, and H. R. Schober, Phys. Rev. Lett. **85**, 4293 (2000).
- [33] A. Rahman, Phys. Rev. **136**, A405 (1964).
- [34] H. Miyagawa and Y. Hiwatari, Phys. Rev. A **44**, 8278 (1991).
- [35] For reviews see M. D. Ediger, Ann. Rev. Phys. Chem. **51**, 99 (2000); H. Sillescu, J. Non-Cryst. Solids **243**, 81 (1999); R. Böhmer, Curr. Opin. Solid State Mat. Sci. **3**, 378 (1998).
- [36] R. Richert, J. Non-Cryst. Solids **172-174**, 209 (1994); R. Richert, J. Phys. Chem. **101**, 6323 (1997); F. R. Blackburn, M. T. Cicerone, G. Hietpas, P. A. Wagner, M. D. Ediger, J. Non-Cryst. Solids **172-174**, 256 (1994); K. Schmidt-Rohr and H. W. Spiess, Phys. Rev. Lett. **66**, 3020 (1991); J. Leisen, K. Schmidt-Rohr and H. W. Spiess, J. Non-Cryst. Solid **172-174**, 737 (1994); A. Heuer, M. Wilhelm, H. Zimmermann and H. W. Spiess, Phys. Rev. Lett. **75**, 2851 (1995); M. T. Cicerone, F. R. Blackburn and M. D. Ediger, J. Chem. Phys. **102**, 471 (1995); M. T. Cicerone and M. D. Ediger, J. Chem. Phys. **103**, 5684 (1995); F. Fujara, B. Geil, H. Sillescu and G. Fleischer, Z. Physik B **88**, 195 (1992); T. Kanaya, U. Buchenau, S. Koizumi, I. Tsukushi and K. Kaji, Phys. Rev. B **61**, R6451 (2000); M. Russina, F. Mezei, R. Lechner, S. Longeville and B. Urban, Phys. Rev. Lett. **84**, 3630 (2000); W. Schmidt, M. Ohl and U. Buchenau, Phys. Rev. Lett. **85**, 5669 (2000); L. F. Cugliandolo, J. Iguain, Phys. Rev. Lett. **85**, 3448 (2000); G. Diezemann, G. Hinze and H. Sillescu, J. Non-Cryst. Solids **307**, 57 (2002); R. E. Courtland and E. R. Weeks, J. Phys.:Condens. Matter **15**, S359 (2003).
- [37] T. Muranaka and Y. Hiwatari, Phys. Rev. E **51**, R2735 (1995); G. Johnson, A. I. Mel'cuk, H. Gould, W. Klein and R. D. Mountain, Phys. Rev. E **57**, 5707 (1998); D. N. Perera and P. Harrowell, Phys. Rev. Lett. **81**, 120 (1998); B. Doliwa and A. Heuer, J. Non-Cryst. Solids **307**, 32 (2002).
- [38] M. M. Hurley and P. Harrowell, Phys. Rev. E **52**, 1694 (1995).
- [39] D. N. Perera and P. Harrowell, J. Chem. Phys. **111**, 5441 (1999).
- [40] B. Doliwa and A. Heuer, Phys. Rev. E **61**, 6898 (2000).
- [41] A. Heuer and K. Okun, J. Chem. Phys. **106**, 6176 (1997); H. R. Schober, C. Gaukel and C. Oligschleger, Prog. Theor. Phys. Suppl. **126**, 67 (1997); R. Yamamoto and A. Onuki, Phys. Rev. E **58**, 3515 (1998); P. H. Poole, C. Donati and S. C. Glotzer, Physica A **261**, 51 (1998); Y. Gebremichael, T. B. Schröder, F. W. Starr, and S. C. Glotzer, Phys. Rev. E **64**, 051503 (2001).
- [42] K. Vollmayr-Lee, W. Kob, K. Binder and A. Zippelius, J. Chem. Phys. **116**, 5158 (2002).
- [43] H. Teichler, Defect Diffus. Forum **143-147**, 717 (1997).
- [44] B. B. Laird and H. R. Schober, Phys. Rev. Lett. **66**, 636 (1991).
- [45] H. R. Schober and B. B. Laird, Phys. Rev. B **44**, 6746 (1991).
- [46] H. R. Schober, C. Oligschleger, and B. B. Laird, J. Non-Cryst. Solids **156**, 965 (1993).
- [47] D. Caprion, M. Kluge and H. R. Schober, MRS Symposia Proceedings No. 754 (Materials Research Society, Pittsburg, 2003).
- [48] H. R. Schober, C. Gaukel, and C. Oligschleger, Progr. Theor. Phys. Suppl. **126**, 67 (1997)
- [49] U. Buchenau, Yu. M. Galperin, V. L. Gurevich, and H. R. Schober, Phys. Rev. E **43**, 5039 (1991); S. D. Benbenek and B. B. Laird, Phys. Rev. Lett. **74**, 936 (1995); H. R. Schober and C. Oligschleger, Phys. Rev. B **53**, 11469 (1996); T. Keyes, G. V. Vijayadamodar, and U. Zurcher, J. Chem. Phys. **106**, 4651 (1997).
- [50] For a review see W. Kob, "Supercooled liquids and glasses," in The Scottish Universities Summer School, *Soft and Fragile Matter - Non-Equilibrium Dynamics, Metastability and Flow*, Edingburgh, 2000.
- [51] J. -P. Bouchaud, L. F. Cugliandolo, J. Kurchan, and M. Mézard, Physica A **226**, 243 (1996); J. -P. Bouchaud, L. F. Cugliandolo, J. Kurchan, and M. Mézard, in *Spin Glasses and Random Fields*, Ed.: A. P. Young (World Scientific, Singapore, 1998).
- [52] L. C. E. Struik, *Physical Aging in Amorphous Polymers and Other Materials*, (Elsevier, Amsterdam, 1978).
- [53] W. Kob and J. -L. Barrat, Phys. Rev. Lett. **78**, 4581 (1997).
- [54] J. -L. Barrat and W. Kob, Europhys. Lett. **46**, 637 (1999).
- [55] S. Sastry, P. G. Debenedetti, F. H. Stillinger, T. B. Schröder, J. C. Dyre, S. C. Glotzer, Physica A **270**, 301 (1999).
- [56] B. Doliwa and A. Heuer, J. Phys.:Condens. Matter **15**, S849 (2003).
- [57] T. B. Schröder, S. Sastry, J. C. Dyre and S. C. Glotzer, J. Chem. Phys. **112**, 9834 (2000).
- [58] B. Doliwa and A. Heuer, Phys. Rev. E **67**, 031506 (2003); B. Doliwa and A. Heuer, e-print cond-mat/0306343 (2003).
- [59] B. Doliwa and A. Heuer, Phys. Rev. E **67**, 030501(R) (2003).
- [60] A. Saksengwijit, B. Doliwa, and A. Heuer, J. Phys.:Condens. Matter **15**, S1237 (2003).

- [61] E. R. Weeks and D. A. Weitz, Chem. Phys. **284**, 361 (2002).
- [62] E. Rabani, J. D. Gezelter, and B. J. Berne, Phys. Rev. Lett. **82**, 3649 (1999).
- [63] E. Rabani, J. D. Gezelter, and B. J. Berne, J. Chem. Phys. **107**, 6867 (1997).
- [64] J. D. Gezelter, E. Rabani, and B. J. Berne, J. Chem. Phys. **110**, 3444 (1999).
- [65] P. Allegrini, J. F. Douglas, and S. C. Glotzer, Phys. Rev. E **60**, 5714 (1999).
- [66] E. Leutheusser, Phys. Rev. A **29**, 2765 (1984); U. Bengtzelius, W. Götze, and A. Sjölander, J. Phys. C **17**, 5915 (1984).
- [67] W. Götze and L. Sjögren, Z. Phys. B **65**, 415 (1987); S. P. Das and G. F. Mazenko, Phys. Rev. A **34**, 2265 (1986); W. Götze and L. Sjögren, J. Phys. C **21**, 3407 (1988); L. Sjögren, Z. Phys. B **79**, 5 (1990); M. Fuchs, W. Götze, S. Hildebrand, and A. Latz, J. Phys.:Condens. Matter **4**, 7709 (1992).
- [68] G. Li, M. Fuchs, W. M. Du, A. Latz, N. J. Tao, J. Hernandez, W. Götze, and H. Z. Cummins, J. Non-Cryst. Solids **172-174**, 43 (1994).
- [69] M. Fuchs, W. Götze, M. R. Mayr, Phys. Rev. E **58**, 3384 (1998).
- [70] M. H. Cohen and G. S. Grest, Phys. Rev. B **20**, 1077 (1979).
- [71] J. T. Bendler and M. F. Shlesinger, J. Phys. Chem **96**, 3970 (1992).
- [72] C. T. Chudley and R. J. Elliott, Proc. Phys. Soc. **77**, 353 (1961); J. W. Haus, K. W. Kehr, and J. W. Lyklema, Phys. Rev. B **25**, 2905 (1982); R. Zwanzig, J. Chem. Phys. **79**, 4507 (1983); J. Machta and R. Zwanzig, Phys. Rev. Lett. **50**, 1959 (1983); T. Odagaki and Y. Hiwatari, Phys. Rev. A **41**, 929 (1990); T. Odagaki and Y. Hiwatari, Phys. A **204**, 464 (1994); J. C. Dyre and J. M. Jacobsen, Phys. Rev. E **52**, 2429 (1995); C. Monthus and J.-P. Bouchaud, J. Phys. A:Math. Gen. **29**, 3847 (1996); J. C. Dyre and J. M. Jacobsen, Chem. Phys. **212**, 61 (1996); A. K. Hartmann and D. W. Heermann, J. Chem. Phys. **108**, 9550 (1998); J. C. Dyre, Phys. Rev. E **59**, 2458 (1999); J. C. Dyre, Phys. Rev. E **59**, 7243 (1999).
- [73] J. C. Dyre, Phys. Lett. **108A**, 457 (1985); T. Odagaki, J. Phys. A:Math. Gen. **20**, 6455 (1987); T. Odagaki, Phys. Rev. B **38**, 9044 (1988); J. C. Dyre, J. Appl Phys. **64**, 2456 (1988); J. C. Dyre and Th. B. Schröder, Phys. Rev. B **54**, 14884 (1996); Th. B. Schröder and J. C. Dyre, Phys. Rev. Lett. **84**, 310 (2000); J. C. Dyre and Th. B. Schröder, Phys. Stat. Sol.(b) **230**, 5 (2002); Th. B. Schröder and J. C. Dyre, Phys. Chem. Chem. Phys. **4**, 3173 (2002).
- [74] H. Miyagawa, Y. Hiwatari, B. Berne, and J. P. Hansen, J. Chem. Phys. **88**, 3879 (1988).
- [75] W. Kob and H.C. Andersen, Phys. Rev. E **51**, 4626 (1995).
- [76] W. Kob and H.C. Andersen, Phys. Rev. Lett. **73**, 1376 (1994); Phys. Rev. E **52**, 4134 (1995).
- [77] The 10 initial configurations differ drastically in their thermal history and are therefore completely independent. They were started at $T = 5.0$ and, after various cooling and reheating periods, were equilibrated at $T = 0.446$. Details can be found in [75, 78].
- [78] T. Gleim and W. Kob, Phys. Rev. Lett. **81**, 4404 (1998).
- [79] As described in Sec. II, we start with the periodically (every 2000 MD steps of step size $\Delta t = 0.02$) stored configurations $\{\mathbf{r}_i(t)\}$ where $t = m \cdot 2000 \cdot 0.02$. For the single particle fluctuations we use the time averages $\overline{\mathbf{r}}_i(m) = \frac{1}{20} \sum_{m'=m-9}^{m'+m+10} \mathbf{r}_i(m')$, their squares $\overline{\mathbf{r}}_i^2(m) = \frac{1}{20} \sum_{m'=m-9}^{m'+m+10} \mathbf{r}_i^2(m')$, and $\sigma_i^2(m) = \overline{\mathbf{r}}_i^2(m) - (\overline{\mathbf{r}}_i(m))^2$ at times $m = 10, 30, \dots$. We first make a preliminary estimate of the fluctuations $\sigma_{i,\text{preest}} = \sqrt{\frac{1}{N_m} \sum_m \sigma_i^2(m)}$ and then obtain the final estimate for the fluctuations $\sigma_{i,\text{est}}$ by redoing the average over σ_i^2 but by averaging only over all $\sigma_i^2(m)$ for which $\sigma_i^2(m) < 5\sigma_{i,\text{preest}}^2$ to roughly exclude jumps from the average.
- [80] We define $\mathbf{r}_i(t)$ to be a spike if $(\mathbf{r}_i(t) - \langle \overline{\mathbf{r}}_i \rangle_f)^2 > 20\langle \sigma_i^2 \rangle_f$ where $\langle \cdot \rangle_f$ is defined as in Sec. VII. Similar to case 1 we say that the spike $\mathbf{r}_i(t)$ returns to the previous average position if $(\mathbf{r}_i(t) - \langle \overline{\mathbf{r}}_i \rangle_i)^2 \leq 5\langle \sigma_i^2 \rangle_i$.
- [81] C. Oligschleger and H. R. Schober, Solid State Commun. **93**, 1031 (1995).
- [82] C. F. Vardeman II and J. D. Gezelter, J. Phys. Chem. A **105**, 2568 (2001).
- [83] E. R. Weeks and H. L. Swinney, Phys. Rev. E **57**, 4915 (1998).
- [84] M. A. Fogleman, M. J. Fawcett and T. H. Solomon, Phys. Rev. E **63**, 020101(R).
- [85] To determine the starting time t_i and ending time t_f of a jump we use an approach similar to our definition for the occurrence of a jump (Eq. (7)). We compare the differences in averaged positions $\Delta \overline{\mathbf{r}}_i(t)$ and the fluctuations $\sigma_{i,\text{est}}$ (see [79]). If a jump has been detected at time $t_{i,\text{detect}}$ (because $|\Delta \overline{\mathbf{r}}_i|^2(t_{i,\text{detect}}) > 20\sigma_{i,\text{est}}^2$) then the starting time t_i is the largest time t for which $|\Delta \overline{\mathbf{r}}_i|^2(t) \leq 5\sigma_{i,\text{est}}^2$ within the boundaries of $t_{i,\text{lowest}} < t_i < t_{i,\text{detect}}$, where in the case of a first jump $t_{i,\text{lowest}}$ corresponds to the beginning of the production run and in the case of the existence of a previous jump with t_f^{prev} then $t_{i,\text{lowest}} = t_f^{\text{prev}}$. Similarly after a jump has started it is detected to be finished at the earliest time $t_{f,\text{detect}}$ for which $|\Delta \overline{\mathbf{r}}_i|^2(t_{f,\text{detect}}) \leq 5\sigma_{i,\text{est}}^2$. The finishing time of the jump t_f is then the maximum of $t_{i,\text{detect}}$ and $t_{f,\text{detect}} - 3200$ where we subtract 3200 ($= 4 \cdot 20 \cdot 2000 \cdot 0.02$) because $\Delta \overline{\mathbf{r}}_i = \overline{\mathbf{r}}_i(t) - \overline{\mathbf{r}}_i(t - 3200)$ (see Eq. (6) and [79]). If the condition for $t_{f,\text{detect}}$ never occurs, then t_f is equal to the length of the simulation run. To determine Δt_b in case 2 of Fig. 2, we use for the first spike the time between the previous t_i and the time of the spike and for successive spikes their time differences.
- [86] F. H. Stillinger and T. A. Weber, J. Chem. Phys. **80**, 4434 (1984); T. A. Weber and F. H. Stillinger, Phys. Rev. B **32**, 5402 (1985).
- [87] In Fig. 19a and Fig. 19b we use the time average windows $\langle \cdot \rangle_{i,f}$. In Fig. 19a we then average over jumps of a certain kind. In the case of a particle with multiple jumps this means that the times after the first jump and before the last jump are counted twice. In Fig. 19b however we compare the behavior of *particles* (instead of jump events) and therefore count these time windows only once.